Design and Analysis of Cylindrical Antiresonant Reflecting Optical Waveguide

C. W. Tee and S. F. Yu, *Senior Member, IEEE*

***Abstract*—A field-transfer matrix method is developed to analyze the modal characteristics of cylindrical multilayered waveguides with axis-symmetric geometry. A new design rule for cylindrical antiresonant reflecting optical waveguides (ARROWs), based on a three-step design process, is also proposed to minimize the radiation loss of the fundamental leaky mode. In addition, a simple approach is suggested to estimate the optimum core diameter of the cylindrical ARROWs for optimum radiation loss and radiation loss margin. Hence, it can be shown that an extra high index cladding layer is good enough to reduce the radiation loss as well as to maintain a reasonably high radiation loss margin in simplified ARROWs for long wavelength application.**

***Index Terms*—Cylindrical antiresonant reflecting optical waveguide, field-transfer matrix theory, leaky modes, radiation loss.**

I. Introduction

RECENTLY, theoretical models have been developed to analyze the modal characteristics of planar antiresonant reflecting optical waveguides (ARROWs) [1]–[4]. However, further extension of these methods to study cylindrical ARROW has not been reported except the use of finite-difference time-domain (FDTD) method [5]. Although the full-vector FDTD method is exact, it requires great computational time and memory for the simulation. Hence, planar approximation is often used to estimate the modal characteristics of cylindrical ARROW vertical cavity surface emitting lasers (VCSELs) [6]. However, the radiation loss margin (i.e., the difference in radiation losses between the fundamental and first order leaky modes) of the cylindrical ARROW may be overestimated by the planar approximation. This is because the radiation loss of the first-order leaky mode calculated from the planar approximation is much higher than that obtained from the exact calculation (see Section II-B for more explanation). Therefore, it is necessary to deduce a more exact and effective method to analyze the modal characteristics of cylindrical ARROWs.

In the design of ARROW VCSELs, the design rule of a planar ARROW is employed to estimate the corresponding optimum thickness of the first cladding layer [6]. This is acceptable because the error that arises from the planar approximation is small. However, the optimum thickness of the second cladding layer obtained from the planar approximation can deviate from the exact solution by more than 1 μm [7]. This is because the leaky modes inside the cylindrical ARROW, which satisfies the Helmholtz equation in polar coordinates, have the properties of Bessel functions. Hence, the nonuniform periodicity (i.e., the periods of the leaky modes in the core and second cladding layers are different; see Section II-C for more explanation) of the leaky modes violates the assumption of the design rule (i.e., requirement of constant lateral wavelength throughout the cavity). Hence, a new design rule is required to be developed for cylindrical ARROW.

Furthermore, the design of ARROW VCSELs requires the devices to have 1) high output power (i.e., large core diameter), 2) stable single-mode operation (i.e., large radiation loss margin) at high power, and 3) low threshold current (i.e., low radiation loss of the fundamental leaky mode). However, the available design of ARROW may not be suitable for long wavelength application as the corresponding radiation loss is very large. Therefore, it is also desired to design a new ARROW structure for long wavelength application.

In this paper, a simple field-transfer matrix model is proposed to study the modal characteristics of the cylindrical multilayered waveguides with axis-symmetric geometry. Furthermore, a new design rule, a rigorous three-step iteration procedure, is proposed to evaluate the optimum thickness of the cladding layers of any cylindrical ARROW structures. A simple approach is also suggested to estimate the optimum core diameter of the cylindrical ARROW for optimum radiation loss and radiation loss margin. In addition, S-ARROW with extra high index cladding layer is proposed for long wavelength application.

II. Theory

In the following paragraphs, a field-transfer matrix model is developed to study the modal characteristics of the cylindrical multilayered waveguides with axis-symmetric geometry. Hence, the field transfer matrix is applied to study the modal characteristics of a cylindrical ARROW. Furthermore, a new design rule, a rigorous three-step design process, is proposed to determine the optimum thickness of the cladding layers of the cylindrical ARROW for minimum radiation loss.

A. Field-Transfer Matrix Model

Fig. 1 shows a portion of the cylindrical multilayered waveguide to be considered in the investigation. It is assumed that the cylindrical multilayered waveguide is divided into $N-1$ concentric rings. Inside the ith concentric ring with uniform refractive index n_i, the corresponding lateral optical field ψ_i, which satisfies the scalar Helmholtz equation in polar coordinate, can be expressed as [8]

$$\psi_i = A_i J_v(\beta_i r) + B_i Y_v(\beta_i r) \tag{1}$$

Manuscript received March 10, 2003; revised August 14, 2003.

The authors are with the School of Electrical and Electronics Engineering, Nanyang Technological University, 639798 Singapore (e-mail: esfyu@ntu.edu.sg).

Digital Object Identifier 10.1109/JLT.2003.820040

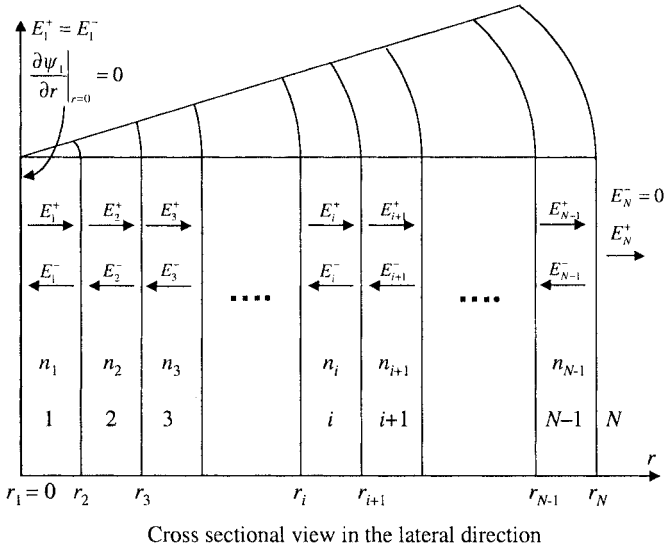

Fig. 1. Cross-sectional view of a cylindrical multilayered waveguide.

where A_i and B_i are some arbitrary constants and J_v and Y_v are vth order Bessel functions of the first and second kind, respectively. $\beta_i = \sqrt{k_0^2(n_i^2 - n_{\text{eff}}^2)}$ is the lateral propagation constant of ψ_i in the ith concentric ring. It is noted that if ψ_i is the bound field, then the effective refractive index n_{eff} of the cylindrical waveguide is real. However, if ψ_i is the leaky field, then n_{eff} is complex. k_0 $(=2\pi/\lambda)$ is the propagation constant and λ is the free space wavelength. Effective index method is used to derive (1) so that the complicated three-dimensional problem is reduced to one-dimensional analysis. This approximation may miss some resonant cavity modes but is a legitimate approximation for a waveguide calculation with polarization restrictions such as ARROW's.

Furthermore, ψ_i along the lateral direction can be expressed in terms of Hankel functions

$$\psi_i = E_i^+ H_v^{(1)}(\beta_i r) + E_i^- H_v^{(2)}(\beta_i r) \tag{2}$$

where E_i^+ (E_i^-) is the amplitude of the outgoing (incoming) lateral optical field inside the ith concentric ring and $H_v^{(1)}$ and $H_v^{(2)}$ are vth order Hankel functions of the first and second kind, respectively. From (2), ψ_i and $\partial\psi_i/\partial r$ can be expressed as a 2×2 matrix as shown in (3) at the bottom of the page. Using (3), a field-transfer matrix, which relates the lateral electric fields in the ith and $i+1$th concentric rings, can be written as shown in (4) at the bottom of the page. ψ at $r = 0$ and $r = r_N$ can be related by multiplying the field-transfer matrices of all the concentric rings, that is

$$\left[\begin{array}{c} \psi_1 \\ \frac{\partial \psi_1}{\partial r} \end{array}\right]\Bigg|_{r=0} = \prod_{i=1}^{N-1} \text{TM}_i \left[\begin{array}{c} \psi_N \\ \frac{\partial \psi_N}{\partial r} \end{array}\right]\Bigg|_{r=r_N} \tag{5}$$

where TM_i is the 2×2 matrix in (4). Hence, the eigenequation of the cylindrical waveguide matrix can be deduced from (5) provided that the appropriate boundary conditions are used.

One of the boundary conditions requires no incoming field beyond $r = r_N$. This implies (6), as shown at the bottom of the page. The boundary condition given in (6), however, cannot be used to evaluate the required eigenequation of the cylindrical waveguide. This is because ψ_N and $\partial\psi_N/\partial r$ are different functions of r. This problem can be solved by using the asymptotic expansions of Hankel functions for large value of r, that is

$$H_v^{(1)}(\beta_N r) \cong \sqrt{\frac{2}{\pi\beta_N r}} \exp\left\{ j\left(\beta_N r - \frac{v\pi}{2} - \frac{\pi}{4}\right)\right\} \tag{7}$$

where $j = \sqrt{-1}$. This approximation is always valid because the condition $\beta_N r > v$ for $0 \le v \le 3$ is satisfied for VCSELs with large aperture (i.e., $r > r_N \sim 9\,\mu$m). Using (7), (6) can be simplified to

$$\left[\begin{array}{c} \psi_N \\ \frac{\partial \psi_N}{\partial r} \end{array}\right]\Bigg|_{r>r_N} \cong \left[\begin{array}{c} 1 \\ j\beta_N \end{array}\right] \psi_N \tag{8}$$

$$\left[\begin{array}{c} \psi_i \\ \frac{\partial \psi_i}{\partial r} \end{array}\right] = \left[\begin{array}{cc} H_v^{(1)}(\beta_i r) & H_v^{(2)}(\beta_i r) \\ \frac{1}{2}\beta_i\left\{H_{v-1}^{(1)}(\beta_i r) - H_{v+1}^{(1)}(\beta_i r)\right\} & \frac{1}{2}\beta_i\left\{H_{v-1}^{(2)}(\beta_i r) - H_{v+1}^{(2)}(\beta_i r)\right\} \end{array}\right] \left[\begin{array}{c} E_i^+ \\ E_i^- \end{array}\right] \tag{3}$$

$$\begin{aligned} \left[\begin{array}{c} \psi_i \\ \frac{\partial \psi_i}{\partial r} \end{array}\right]\Bigg|_{r=r_i} = {} & \left[\begin{array}{cc} H_v^{(1)}(\beta_i r_i) & H_v^{(2)}(\beta_i r_i) \\ \frac{1}{2}\beta_i\left\{H_{v-1}^{(1)}(\beta_i r_i) - H_{v+1}^{(1)}(\beta_i r_i)\right\} & \frac{1}{2}\beta_i\left\{H_{v-1}^{(2)}(\beta_i r_i) - H_{v+1}^{(2)}(\beta_i r_i)\right\} \end{array}\right] \\ & \times \left[\begin{array}{cc} H_v^{(1)}(\beta_i r_{i+1}) & H_v^{(2)}(\beta_i r_{i+1}) \\ \frac{1}{2}\beta_i\left\{H_{v-1}^{(1)}(\beta_i r_{i+1}) - H_{v+1}^{(1)}(\beta_i r_{i+1})\right\} & \frac{1}{2}\beta_i\left\{H_{v-1}^{(2)}(\beta_i r_{i+1}) - H_{v+1}^{(2)}(\beta_i r_{i+1})\right\} \end{array}\right]^{-1} \\ & \times \left[\begin{array}{c} \psi_{i+1} \\ \frac{\partial \psi_{i+1}}{\partial r} \end{array}\right]\Bigg|_{r=r_{i+1}} \end{aligned} \tag{4}$$

$$\left[\begin{array}{c} \psi_N \\ \frac{\partial \psi_N}{\partial r} \end{array}\right]\Bigg|_{r>r_N} = \left[\begin{array}{cc} H_v^{(1)}(\beta_N r) & H_v^{(2)}(\beta_N r) \\ \frac{1}{2}\beta_N\left\{H_{v-1}^{(1)}(\beta_N r) - H_{v+1}^{(1)}(\beta_N r)\right\} & \frac{1}{2}\beta_N\left\{H_{v-1}^{(2)}(\beta_N r) - H_{v+1}^{(2)}(\beta_N r)\right\} \end{array}\right] \left[\begin{array}{c} E_N^+ \\ 0 \end{array}\right] \tag{6}$$

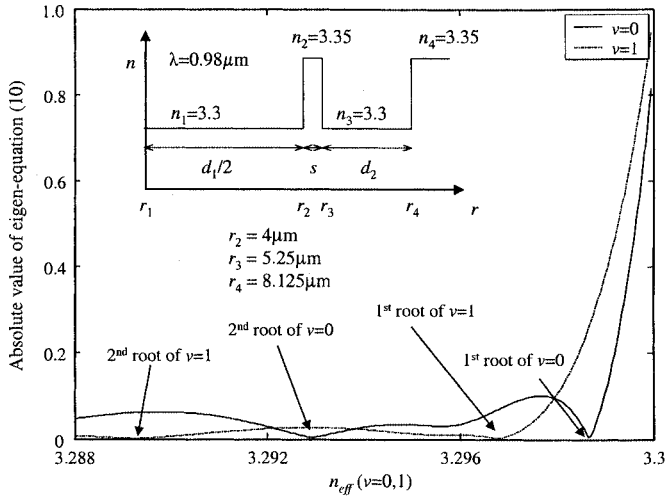

Fig. 2. Plot of relative absolute value of (10) versus $n_{\rm eff}(\sim n_{\rm Re})$. The four approximated roots are labeled as fundamental mode (first root of v = 0), first-order mode (first root of v = 1), second-order mode (second root of v = 0), and third-order mode (second root of v = 1). Inset is the refractive index profile of ARROW.

so that both ψ_N and $\partial\psi_N/\partial r$ can be related by a constant. The other boundary condition requires $\partial\psi_1/\partial r = 0$ at $r = 0$. Using these boundary conditions, (5) can be simplified to

$$\left.\begin{bmatrix}\psi_1\\ 0\end{bmatrix}\right|_{r=0} = \prod_{i=1}^{N} \mathrm{TM}_i \left.\begin{bmatrix}\psi_N\\ j\beta_N\psi_N\end{bmatrix}\right|_{r>r_N} = \left.\begin{bmatrix}\mathrm{tm}_{11} & \mathrm{tm}_{12}\\ \mathrm{tm}_{21} & \mathrm{tm}_{22}\end{bmatrix}\begin{bmatrix}\psi_N\\ j\beta_N\psi_N\end{bmatrix}\right|_{r>r_N}. \quad (9)$$

As a result, the required eigenequation can be expressed as

$$\eta(n_{\rm eff}) \equiv \mathrm{tm}_{21} + j\beta_N \mathrm{tm}_{22} = 0 \quad (10)$$

with which the effective refractive indexes of bound or leaky modes supported by any cylindrical waveguides can be determined. The eigenvalues of (10) (i.e., the roots of $\eta(n_{\rm eff}) = 0$) can be calculated by varying $n_{\rm eff}$.

B. Example—Modal Characteristics of a Cylindrical ARROW

Fig. 2 shows the schematic of a cylindrical ARROW to be investigated. The dimensions of the cylindrical ARROW are selected so that the fundamental leaky mode has the minimum radiation loss. The procedures to calculate $n_{\rm eff}$ and the lateral field profile of the leaky modes by (10) can be summarized as follows:

1) It is noted that $n_{\rm eff}$ of the leaky modes is complex and can be expressed as $n_{\rm eff} = n_{\rm Re} + jn_{\rm Im}$, where $n_{\rm Re}$ and $n_{\rm Im}$ are real numbers. If only low-loss leaky modes are considered in the analysis, it is possible to assume $n_{\rm eff} \sim n_{\rm Re}$. Hence, the approximated value of $n_{\rm eff}$ for the leaky modes can be obtained from the minimum points (i.e., close to zero) of $|\eta|$ versus $n_{\rm Re}$ curve (see also Fig. 2).
2) The exact value of $n_{\rm eff}$ can be obtained by solving $\eta(n_{\rm eff}) = 0$ numerically using $n_{\rm eff} \sim n_{\rm Re}$ as the initial guess. Once $n_{\rm eff}$ is obtained, β_i of all the concentric rings can be deduced.
3) The intensity profile of the leaky modes can be calculated by

$$|\psi_i|^2 = \left|E_i^+ H_v^{(1)}(\beta_i r) + E_i^- H_v^{(2)}(\beta_i r)\right|^2 \quad (11)$$

where $E_1^+ = E_1^-$ (=arbitrary number) is assumed in the first concentric ring. The other amplitudes of the electric fields in the subsequent concentric rings can also be evaluated by using the continuity condition of ψ_i and its derivative at all the interfaces. From (3), it can be shown that the required field transfer matrix can be written as shown in (12) at the bottom of the page.

Fig. 3(a) plots the intensity profiles of the fundamental and first-order leaky modes in the cylindrical ARROW. The corresponding magnifications for the region $r \geq 4\,\mu$m are also shown in Fig. 3(b). It is observed that the fundamental mode vanishes at positions r_2 and r_4 (i.e., nodes). This is due to the destructive interference between the outgoing and incoming fields at these locations. Constructive interference of both incoming and outgoing fields is also occurred at the position r_3 so that an antinode is formed. On the other hand, the nodes of the first-order mode deviate from the positions r_2 and r_4, while the antinode moves into the second cladding layer. Hence, only the fundamental leaky mode satisfies the antiresonant condition, and the corresponding radiation loss is minimized.

Fig. 4(a) plots the intensity profile of the fundamental and first-order leaky modes estimated from the planar approximation. The corresponding magnifications for the region $r \geq 4\,\mu$m are also shown in Fig. 4(b). In the calculation, the optimum dimensions of the cylindrical ARROW are obtained from the planar approximation with $r_2 = 4.0, r_3 = 5.3268$, and $r_4 = 9.3268\ \mu$m. The profile of the fundamental leaky mode estimated from the planar approximation is similar to that obtained from our more accurate calculation. As a result, the radiation loss computed from both methods can be quite close to each other. However, it is observed that the profiles of the first-order leaky mode obtained from both methods are quite different. The magnitude of the antinode of the first-order leaky mode inside the second cladding layer calculated from the planar approximation is much higher than that obtained from our field transfer

$$\begin{bmatrix}E_{i+1}^+\\ E_{i+1}^-\end{bmatrix} = \begin{bmatrix} H_v^{(1)}(\beta_{i+1}r_{i+1}) & H_v^{(2)}(\beta_{i+1}r_{i+1})\\ \frac{1}{2}\beta_{i+1}\left\{H_{v-1}^{(1)}(\beta_{i+1}r_{i+1}) - H_{v+1}^{(1)}(\beta_{i+1}r_{i+1})\right\} & \frac{1}{2}\beta_{i+1}\left\{H_{v-1}^{(2)}(\beta_{i+1}r_{i+1}) - H_{v+1}^{(2)}(\beta_{i+1}r_{i+1})\right\}\end{bmatrix}^{-1} \times \begin{bmatrix} H_v^{(1)}(\beta_i r_{i+1}) & H_v^{(2)}(\beta_i r_{i+1})\\ \frac{1}{2}\beta_i\left\{H_{v-1}^{(1)}(\beta_i r_{i+1}) - H_{v+1}^{(1)}(\beta_i r_{i+1})\right\} & \frac{1}{2}\beta_i\left\{H_{v-1}^{(2)}(\beta_i r_{i+1}) - H_{v+1}^{(2)}(\beta_i r_{i+1})\right\}\end{bmatrix}\begin{bmatrix}E_i^+\\ E_i^-\end{bmatrix}. \quad (12)$$

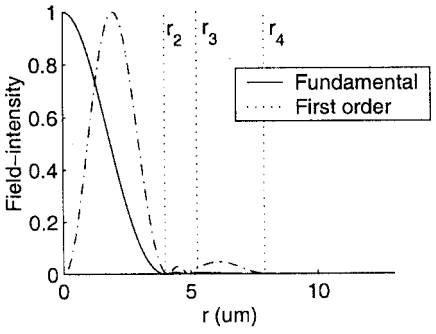

(a)

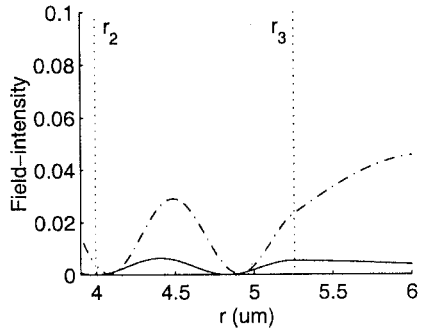

(b)

Fig. 3. (a) Intensity profiles of fundamental and first-order leaky modes calculated by transfer matrix method. (b) Magnified view of (a).

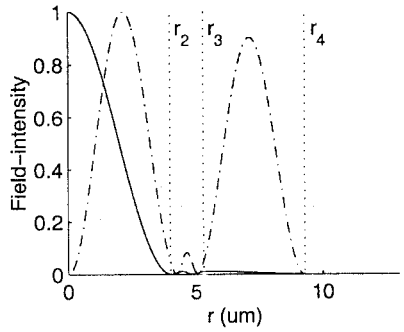

(a)

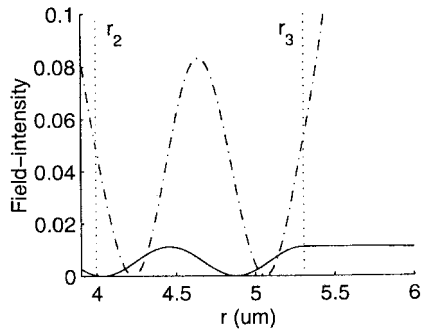

(b)

Fig. 4. (a) Intensity profiles of fundamental and first-order leaky modes calculated by planar approximation. (b) Magnified view of (a).

matrix method. This is because the envelope of the first-order leaky mode calculated from the planar approximation is almost independent on r (i.e., properties of cosine/sine functions) but that obtained from our field-transfer matrix method is inversely proportional to the square root of r [i.e., properties of Bessel functions, see (7)]. As the radiation loss of the first-order leaky mode is proportional to the magnitude of the field distribution inside the second cladding layer, the planar approximation will overestimate the radiation loss of the first-order mode as well as the radiation loss margin of the cylindrical ARROW. The calculation of first-order leaky mode given in [6, Fig. 4(b)] shows that the magnitudes of the antinodes inside the core and second cladding layer are close to each other. Hence, it is believed that the planar approximation was used in their design of cylindrical ARROW.

C. Design Rule of Cylindrical ARROW Using Field-Transfer Matrix

According to planar approximation, the thickness of the second cladding layer $d_2(= r_4 - r_3)$ should be equal to the radius of the core region r_2 $(=d_1/2)$ [6]. This is because the lateral wavelength of the leaky modes should be uniform throughout the ARROW structure (i.e., properties of cosine/sine functions) in order to obtain antiresonant condition [see Fig. 4(a)]. Similar antiresonant condition is also observed in our calculation using field-transfer matrix method, but the lateral wavelength of the leaky modes inside the second cladding layer is shorter than that inside the core region [see Fig. 3(a)]. This is again due to the nonuniform periodicity of Bessel function, as the period of the standing wave within the core and second cladding layers is equal to 2.403 and $\pi/2$, respectively. These correspond to the separation between the center and first root of $J_0(\zeta)$ (i.e., between r_1 and r_2) as well as the separation between the second root of $J_1(\zeta)$ and third root $J_0(\zeta)$ (i.e., between r_3 and r_4). Hence, if $d_1/2 = 4\ \mu$m, then d_2 should be equal to $d_2 = (2.403/\pi/2)^{-1} \times d_1/2 = 2.61\ \mu$m, which is close to our more exact calculation and is much shorter than that obtained from the planar approximation. It must be noted that the error arising from the estimation of d_2 using planar approximation will not reduce with the increase of d_1. This is because the ratio between the lateral wavelength inside the core and second cladding layer of the cylindrical ARROW is independent of the diameter of the core region, so that the ratio $d_2/d_1 = \pi/(4 \times 2.403)$ is a constant.

Hence, a new design rule of cylindrical ARROW, which involves a three-step design process, is proposed. The three-step design process consists of 1) a rough estimation of waveguide dimensions (using the approximation $\psi \propto J_v(\beta r)$), 2) a better iterative approximation method [using $\psi \propto AJ_v(\beta r) + BY_v(\beta r)$ or (2)] and 3) an iterative process incorporated with field-transfer matrix. The reasons to go through these lengthy design procedures is because in cylindrical structure, the analytical expression for optimum thickness of cladding layers cannot be deduced explicitly [3]. Apart from this, the convergent efficiency of the field-transfer matrix is dependent on the initial guess of n_{eff} and the waveguide dimensions.

If only fundamental leaky mode is considered in the analysis, the three-step design process can be written as follows.

First, it can be shown that due to the axis-symmetric properties of the cylindrical ARROW, the corresponding

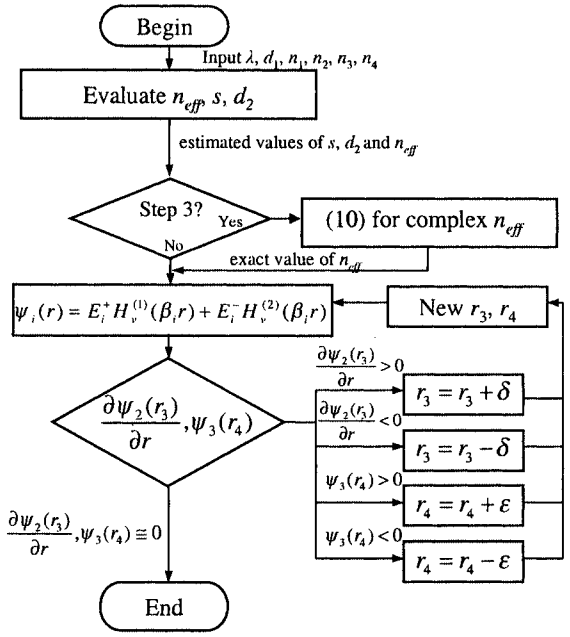

Fig. 5. A three-step design process for cylindrical ARROW. The design process requires the free-space wavelength λ, core diameter d_1, and refractive indexes of the four layers (n_1, n_2, n_3, n_4) of the ARROW as the inputs. If the radiation loss of the fundamental leaky mode is high, Step 3) will be executed using the field-transfer matrix to solve for the exact value of $n_{\rm eff}$.

field profile of the fundamental leaky mode can be roughly approximated by the Bessel function of the first kind, that is, $\psi \propto J_0(\beta r)$. Using the fact that the optimum dimensions of the cylindrical ARROW are obtained when the antinode (nodes) of the fundamental leaky mode is (are) located at r_3 (r_2 and r_4), the analytical expressions for the optimum dimensions of the ARROW structure can be deduced (see also Fig. 3). The $n_{\rm eff}$ of the cylindrical ARROW can be estimated by recognizing the position of node at r_2, which corresponds to the first root of $J_0(\beta r)$. As a result, $n_{\rm eff}$ can be approximated by $n_{\rm eff} \cong \sqrt{n_1^2 - (0.7655\lambda/d_1)^2}$, where $d_1 = 2r_2$. Again, by recognizing the position of antinodes at r_3, the thickness of the first cladding layer s $(=r_3 - r_2)$ can be obtained from the second root of $J_1(\beta r)$ (or $\partial\psi/\partial r = 0$ at r_3). Hence, s can be expressed as $s \cong 0.7338\lambda/\sqrt{n_2^2 - n_{\rm eff}^2}$. It is noted from Fig. 3 that the field intensity has another node at r_4, which corresponds to the third root of $J_0(\beta r)$. Therefore, the second cladding layer thickness d_2 $(=r_4 - r_3)$ can be written as $d_2 \cong 0.2607\lambda/\sqrt{n_3^2 - n_{\rm eff}^2}$.

Second, Fig. 5 shows the proposed iteration process used to deduce s and d_2 of the cylindrical ARROW. In this calculation, (2) is used to describe the lateral field profiles of the leaky modes and the approximated values of s and d_2 can be obtained from Step 1) as the initial guess of this iteration process. The purpose of this iteration process is to find a better approximation to s and d_2 than that obtained from Step 1) so that the antinode (node) of the leaky modes calculated from (2) can be accurately positioned at r_3 (r_4).

For low-loss cylindrical ARROW, the values of s and d_2 calculated by the above iteration process can be quite close to the optimum dimensions, so the use of transfer matrix method can be bypassed. However, if the radiation losses of the leaky modes are large (e.g., ARROWs operating at long wavelength), the assumption $n_{\rm eff} \sim n_{\rm Re}$ will not be satisfied anymore. Therefore, an additional step [i.e., Step 3) as shown below] is required.

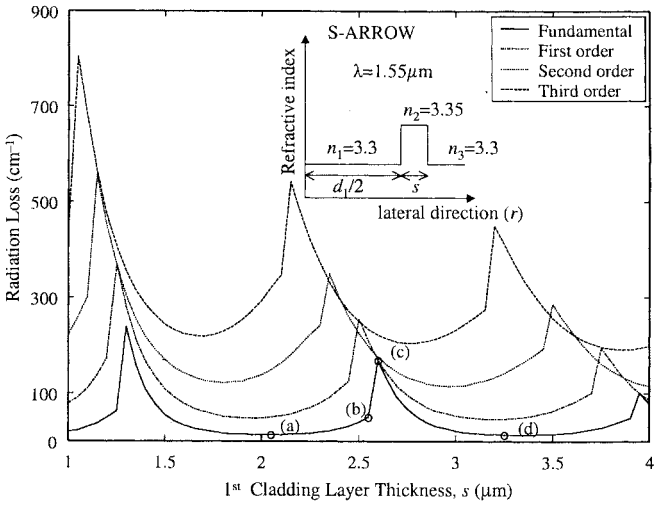

Fig. 6. Radiation losses versus thickness of the first cladding layer s of the S-ARROW. Insert is the refractive index profile of S-ARROW.

Third, the modified iteration process is also illustrated in Fig. 5. In the process, the exact value of $n_{\rm eff}$ is calculated by (10). The convergent efficiency of the iteration process can be maximized provided that the values of $n_{\rm eff}, s$, and d_2 obtained from Step 2) are used as the initial guess. However, the magnitudes of the fine-tuning steps δ and ε should be small enough (i.e., $<10^{-3}$ μm) to maintain convergence of the iteration process if the radiation losses of the leaky modes are large.

From above, the values of s and d_2 can be optimized for a given value of d_1.

III. Numerical Results

In the following analysis, the modal characteristics of S-ARROW and ARROW operating at long wavelength (i.e., 1.55 μm) are studied. It is suggested that the optimum value of d_1 can be estimated by minimizing the ratio between the radiation loss of fundamental leaky mode and radiation loss margin of the waveguides. It is also shown that these conventional ARROW structures may not be suitable to realize long-wavelength VCSELs due to the high radiation loss of the fundamental leaky mode. Therefore, it is proposed to introduce an extra high index cladding layer to S-ARROW in order to reduce the radiation loss and to increase the radiation loss margin.

A. Modal Characteristics of Cylindrical S-ARROW and ARROW

Fig. 6 plots the radiation losses versus the thickness of the first cladding layer s for the four leaky modes (which have the lowest radiation losses) of S-ARROW with r_2 $(=d_1/2)$ $= 4$ μm. It is observed that the shapes of the four curves are similar except the values of the radiation losses are different. The fun-

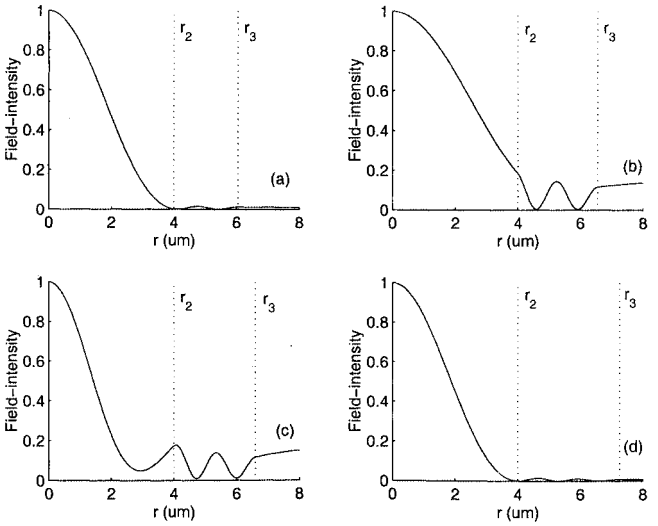

Fig. 7. Intensity profile of the fundamental leaky modes obtained from Fig. 7 with s set to (a) 2.025 μm, (b) 2.575 μm, (c) 2.6 μm, and (d) 3.325 μm.

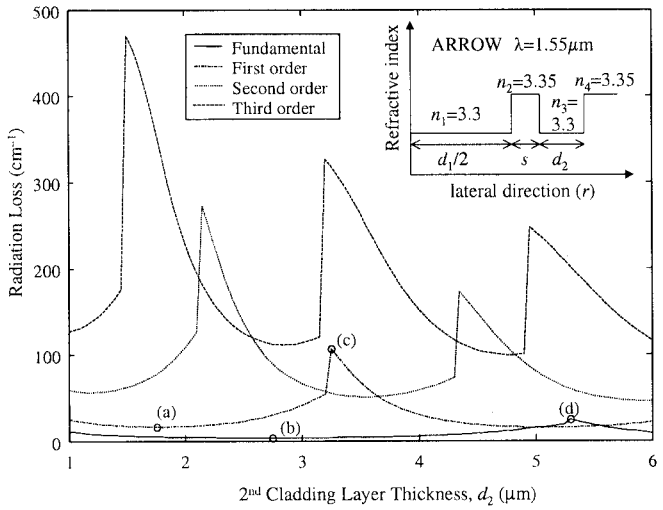

Fig. 9. Radiation losses versus thickness of the second cladding layer d_2 of the ARROW. Insert is the refractive index profile of ARROW.

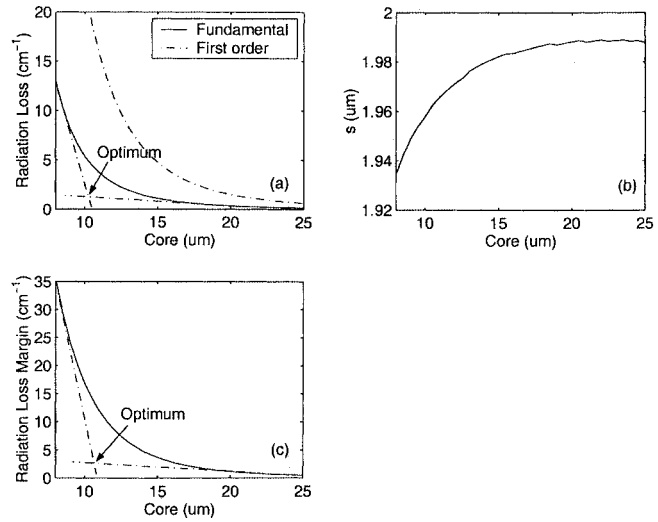

Fig. 8. (a) Radiation losses of fundamental and first-order leaky mode versus d_1, (b) the thickness of the first cladding layers s versus d_1, and (c) radiation loss margin versus d_1.

damental mode has the lowest radiation loss because it has the largest (longest) value of n_{Re} (lateral wavelength). Therefore, the optimum value of s for the fundamental leaky mode is the longest. The intensity profiles of the fundamental leaky mode at different values of s are shown in Fig. 7. It is observed that the maximum (minimum) radiation loss is due to constructive (destructive) interference or antinode (node) at the interface r_2.

Fig. 8 plots (a) the radiation losses of the fundamental and first-order leaky modes versus d_1, (b) the optimum thickness of first cladding layer s versus d_1, and (c) the radiation loss margin versus d_1. In the calculation, the value of s is optimized for the fundamental leaky mode. It is observed that the radiation losses and radiation loss margin are reduced with the increase in d_1. On the other hand, the optimum value of s increases along with d_1 so that the antiresonant condition of the fundamental leaky mode can be satisfied. It is noted that larger d_1 reduces the radiation loss of the fundamental leaky mode, but with the expense of decreasing the high radiation loss margin. Therefore, it is necessary to deduce an optimum value of d_1 in order to maintain the balance between the radiation loss and radiation loss margin (i.e., to minimize the ratio between the radiation loss and radiation loss margin). As a result, the waveguide can have small enough radiation loss (large enough radiation loss margin) to minimize the threshold current (suppress the higher order leaky modes) in VCSELs. As shown in Fig. 8(a) and (c), the optimum value of d_1 can be obtained from the interception of the interpolations from two straight lines tangential to the curves at $d_1 = 7$ μm and $d_1 = 25$ μm. It is found that the optimum value of d_1 is around 10 μm, and the corresponding values of radiation loss and radiation loss margin are around 6 and 15 cm^{-1}, respectively.

Fig. 9 plots the radiation losses of the four leaky modes versus the thickness of the second cladding layer d_2 of ARROW. In the calculation, r_2 $(= d_1/2)$ is again set to 4 μm and s is optimized for the antiresonant condition of the leaky modes. Fig. 10 shows the intensity profiles of ARROW with different values of d_2. It is observed that the increase in radiation loss is due to the increase in the magnitude of antinode inside the second cladding layer (i.e., as indicated by an arrow). The modal characteristics of ARROW with different values of d_1 are also investigated. Fig. 11 plots (a) the radiation losses of the fundamental and first-order leaky modes versus d_1, (b) the optimum thickness of first cladding layer s versus d_1, (c) the optimum thickness of the third cladding layer d_2 versus d_1, and (d) the radiation loss margin versus d_1. From Fig. 11(a) and (d), it is found that the optimum value of d_1 is about 10 μm. Furthermore, the corresponding radiation loss and radiation loss margin are found to be 1.5 and 14 cm^{-1}, respectively. Hence, it is shown that ARROW has better threshold performance than that of S-ARROW because the radiation loss of the fundamental leaky mode of ARROW is much smaller than that of S-ARROW but the radiation loss margin of ARROW and S-ARROW is similar at $d_1 = 10$ μm.

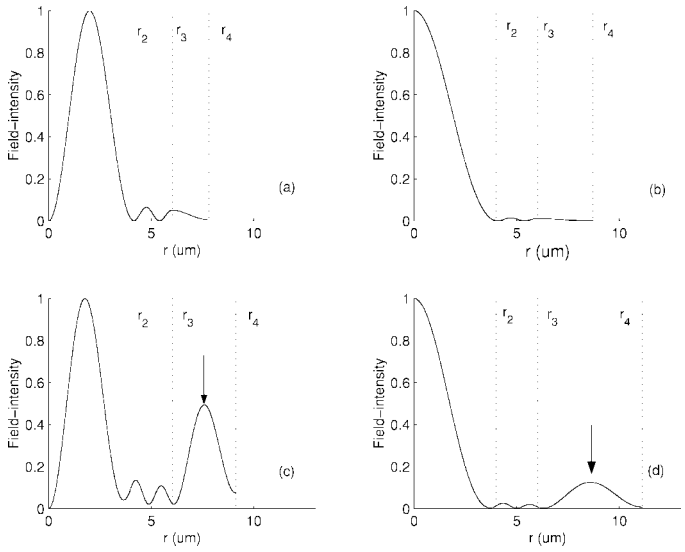

Fig. 10. Intensity profiles of the fundamental leaky mode with d_2 set to (a) 2.875 μm and (b) 5.8 μm. Intensity profiles of the first-order leaky modes with d_2 set to (c) 1.8 μm and (d) 3.7 μm.

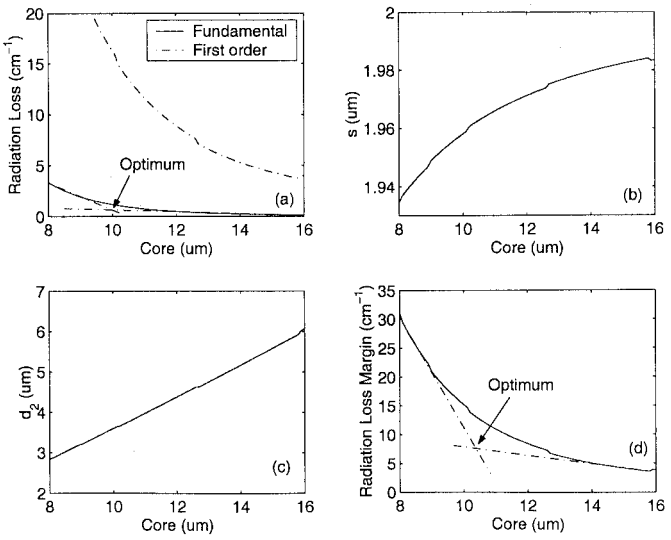

Fig. 11. (a) The radiation loss of fundamental and first-order mode of ARROW plotted against core diameter d_1. (b) The thickness of the high-index cladding layers s plotted against d_1. (c) The thickness of second cladding layer d_2, versus d_1. (d) Radiation loss margin versus d_1.

From above analysis, it is noted that ARROW may be a good choice to realize long-wavelength VCSELs. However, for ARROW with $d_1 = 10$ μm, the corresponding radiation loss of the fundamental leaky mode is 1.5 cm^{-1}, which is not small enough to realize high-performance VCSELs [6]. Although further increase in d_1 can reduce the radiation loss of the fundamental leaky mode, the radiation loss margin will also decrease. Therefore, an extra cladding layer is proposed to reduce (maintain) the radiation loss (radiation loss margin) of the S-ARROW and ARROW. In the following paragraphs, the modal characteristics of S-ARROW and ARROW with an extra high index cladding layer are investigated.

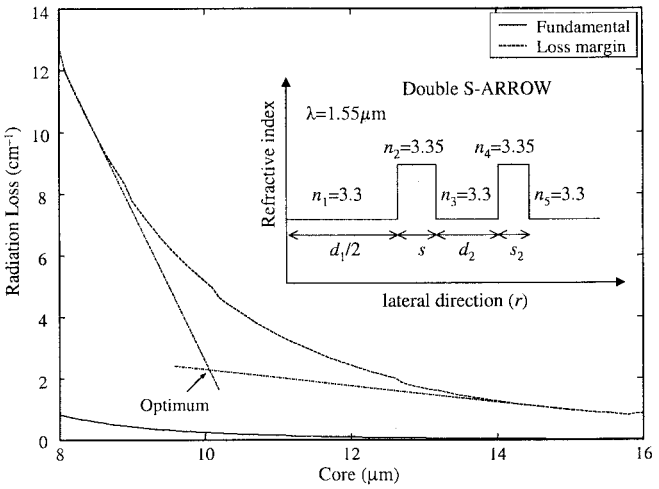

Fig. 12. Plots of radiation loss of fundamental modes (solid line) and radiation loss margin (dashed line) of double S-ARROW versus d_1. Insert is the refractive index profile of the double S-ARROW.

B. Modal Characteristics of Cylindrical Double S-ARROW and Double-ARROW

Fig. 12 shows the schematic of double S-ARROW. In the design of double S-ARROW, the thickness of the third cladding layer s_2 has to be taken into the iteration process. In order to perform Step 1) of the design rule, the analytical expression of s_2 has to be deduced for the calculation process. Using the approximation $\psi \propto J_v(\beta r)$, s_2 can be expressed as

$$s_2 \cong 0.7433\lambda \Big/ \sqrt{n_4^2 - n_{\text{eff}}^2}\,. \tag{13}$$

Using (13), Steps 2) and 3) of the three-step design process can also be performed and the optimum thickness of s_2 can be evaluated iteratively. In the analysis of the radiation losses of the double S-ARROW versus s_2, the values of s and d_2 are optimized for the fundamental leaky mode to achieve antiresonant condition. The antiresonant condition established within the first cladding layer is also maintained inside the third cladding layer of the double S-ARROW. Hence, the plots of s, s_2, and d_2 versus d_1 are not repeated. Fig. 12 also shows the variation of radiation loss (of fundamental leaky mode) and radiation loss margin versus d_1. It is observed that the optimum value of d_1 is around 10 μm. The corresponding radiation loss and radiation loss margin are found to be 0.4 and 5.5 cm^{-1}, respectively. It is noted that the fundamental leaky mode of double S-ARROW has much lower radiation loss than that of ARROW-type structures as described in Section III-A and the value of radiation loss margin is still large enough to discriminate higher order leaky modes in VCSELs. Please be noted that in the design of 0.98-μm ARROW-type VCSELs with $d_1 = 8$ μm, the required optimum radiation loss and radiation loss margin are 1 and 5 cm^{-1}, respectively [6].

Fig. 13 shows the schematic of double ARROW. In the calculation, the thickness of the third cladding layer s_2, as well as the thickness of the fourth cladding layer d_3, of double ARROW

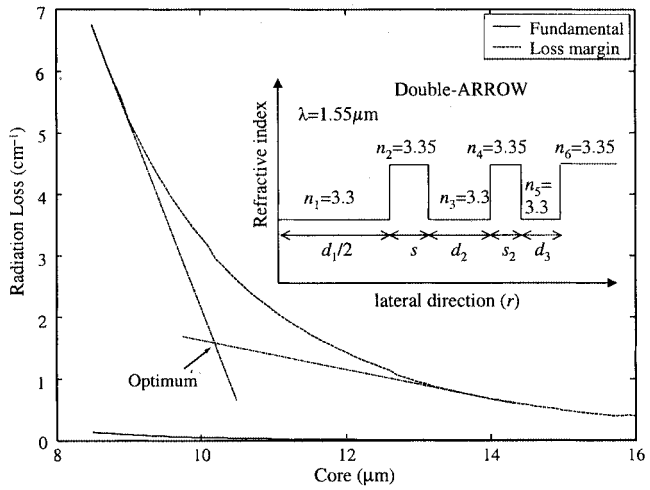

Fig. 13. Plots of radiation loss of fundamental modes (solid line) and radiation loss margin (dashed line) of double ARROW versus d_1. Insert is the refractive index profile of the double ARROW.

has to be taken in the iteration process. It can be shown that the approximated expression of d_3 can be written as

$$d_3 \cong 0.2558\lambda \Big/ \sqrt{n_5^2 - n_{\text{eff}}^2}\ . \tag{14}$$

Using (14), the optimum thickness of d_3 can be evaluated iteratively. In the study of double ARROW, the values of s, d_1, d_2, and s_2 are optimized for the fundamental leaky mode to achieve antiresonant condition. Hence, antiresonant condition of the fundamental leaky mode can be enhanced by the extra cladding layer, so that the radiation loss of double-ARROW is lower than that of double S-ARROW. From Fig. 13, it can be shown that the optimum d_1 of double-ARROW is again 10 μm and the corresponding radiation loss and radiation loss margin are found to be 0.04 and 3.5 cm^{-1}, respectively. Hence, it is proven that extra cladding layer in ARROW can significantly reduce the radiation loss of the fundamental leaky mode to a very low value.

IV. Discussion and Conclusion

In the analysis of cylindrical ARROW [6], it is believed that the planar approximation can be used to estimate the optimum thickness of the cladding layers. The argument is that if the ARROW structures have large d_1, the corresponding leaky modes can be approximately described by cosine and sine functions. This assumption is valid as far as the field profile of leaky modes far away from the core region are concerned and this is the reason for us to use (7) to approximate optical field in the cylindrical ARROW at $r \geq r_N$. However, using planar approximation to estimate the optimum dimensions of cylindrical ARROW is still not appropriate. The reasons have been explained in Section II-B and -C. This is because 1) the leaky modes have nonuniform lateral wavelength and 2) the envelope of the leaky modes reduces along the lateral direction. On the other hand, the leaky modes describe by planar approximation assumed that the lateral wavelengths between the core and second cladding layers are equal in order to satisfy the antiresonant condition. In addition, the magnitude of antinodes of the first-order leaky mode inside the second cladding layer is close to that inside the core region. Therefore, the use of planar approximation will overestimate the radiation loss margin of the cylindrical ARROW and the overestimation cannot be reduced by the increase of core diameter.

In conclusion, a simple field transfer matrix is developed to analyze the modal characteristics of cylindrical ARROW. A new design rule is proposed to optimize the dimension of the cylindrical ARROW. Hence, it is found that the double S-ARROW with $d_1 = 10$ μm is the best choice to realize long-wavelength VCSELs. This is because the corresponding radiation loss (radiation loss margin) is low (high) enough to minimize threshold current (suppress higher order leaky modes) of VCSELs. In addition, the waveguide structure of double S-ARROW is less complicated than that of double ARROW.

References

[1] M. A. Duguay, Y. Kokubun, T. L. Koch, and L. Pfeiffer, "Antiresonant reflecting optical waveguides in SiO_2-Si multilayer structures," *Appl. Phys. Lett.*, vol. 49, no. 1, pp. 13–15, July 1986.

[2] T. Baba and Y. Kokubun, "Dispersion and radiation loss characteristics of antiresonant reflecting optical waveguides—Numerical results and analytical expressions," *IEEE J. Quantum Electron.*, vol. 28, pp. 1689–1700, July 1992.

[3] J. M. Kubica, "A rigorous design method for antiresonant reflecting optical waveguides," *IEEE Photon. Technol. Lett*, vol. 6, pp. 1460–1462, Dec. 1994.

[4] W. Huang, R. M. Shubair, A. Nathan, and Y. L. Chow, "The modal characteristics of ARROW structures," *J. Lightwave Technol.*, vol. 10, pp. 1015–1022, Aug. 1992.

[5] T. W. Lee, S. C. Hagness, D. Zhou, and L. J. Mawst, "Modal characteristics of ARROW-type vertical cavity surface emitting lasers," *IEEE Photon. Technol. Lett.*, vol. 13, pp. 770–772, Aug. 2001.

[6] D. Zhou and L. J. Mawst, "High power single-mode antiresonant reflecting optical waveguide-type vertical surface emitting lasers," *IEEE J. Quantum Electron.*, vol. 38, pp. 1599–1606, Dec. 2002.

[7] C. W. Tee, C. C. Tan, and S. F. Yu, "Design of antiresonant reflecting optical waveguide-type vertical cavity surface emitting lasers using transfer matrix method," *IEEE Photon. Technol. Lett.*, pp. 1231–1233, Sept. 2003.

[8] C. C. Davis, *Lasers and Electro-Optics: Fundamentals and Engineering.* Cambridge, U.K.: Cambridge Univ. Press, 1996.

C. W. Tee, photograph and biography not available at the time of publication.

S. F. Yu (SM'03), photograph and biography not available at the time of publication.